

Directional Persistence of EGF-Induced Cell Migration Is Associated with Stabilization of Lamellipodial Protrusions

Brian D. Harms,* Gina M. Bassi,* Alan Rick Horwitz,† and Douglas A. Lauffenburger*†

*Department of Chemical Engineering, †Department of Biology, and Biological Engineering Division, Massachusetts Institute of Technology, Cambridge, Massachusetts 02139; and ‡Department of Cell Biology, University of Virginia, Charlottesville, Virginia 22908

ABSTRACT Migrating cells can sustain a relatively constant direction of lamellipodial protrusion and locomotion over timescales ranging from minutes to hours. However, individual waves of lamellipodial extension occur over much shorter characteristic times. Little understanding exists regarding how cells might integrate biophysical processes across these disparate timescales to control the directional persistence of locomotion. We address this issue by examining the effects of epidermal growth factor (EGF) stimulation on long-timescale directional persistence and short-timescale lamellipodial dynamics of EGF receptor-transfected Chinese hamster ovary cells migrating on fibronectin-coated substrata. Addition of EGF increased persistence, with the magnitude of increase correlating with fibronectin coating concentration. Kymographic analysis of EGF-stimulated lamellipodial dynamics revealed that the temporal stability of lamellipodial protrusions similarly increased with fibronectin concentration. A soluble RGD peptide competitor reduced both the persistence of long-timescale cell paths and the stability of short-timescale membrane protrusions, indicating that cell-substratum adhesion concomitantly influences lamellipodial dynamics and directional persistence. These results reveal the importance of adhesion strength in regulating the directional motility of cells and suggest that the short-timescale kinetics of adhesion complex formation may play a key role in modulating directional persistence over much longer timescales.

INTRODUCTION

Cell migration plays an essential role in normal and pathological processes such as embryonic morphogenesis (Keller, 2002), inflammation and the immune response (Hart, 2002), wound healing (Martin, 1997), metastatic cancer (Kassis et al., 2001), rheumatoid arthritis (Szekanecz and Koch, 2000), and atherosclerosis (Kraemer, 2000). Critical to both normal and dysregulated motility is the adhesive interaction between cells and substratum. Formation of adhesions at the leading edge of migrating cells stabilizes lamellipodial protrusions, whereas movement of the cell body requires both generation of traction force against the substratum and the regulated release of adhesions at the cell rear (Lauffenburger and Horwitz, 1996; Mitchison and Cramer, 1996).

Migrating cells follow a persistent random walk model parameterized by both cell speed (S) and directional persistence time (P). Persistence characterizes the average time between significant changes in the direction of a cell's translocation (Dunn, 1983; Gail and Boone, 1970; Othmer et al., 1988). The existence of a biphasic relationship between cell adhesion strength and speed is well-established, with maximal speed occurring at intermediate levels of adhesion (DiMilla et al., 1993; Goodman et al., 1989; Maheshwari et al., 1999; Palecek et al., 1997). In contrast, previous studies of the correlation between cell adhesion and persistence are contradictory, with both biphasic and inverted biphasic relationships having been reported

(DiMilla et al., 1993; Ware et al., 1998). As such, the adhesive regulation of directional persistence is poorly understood and requires further study.

Because a cell must extend an adherent new leading lamellipod to change its direction of locomotion, the relationship between cell-substratum adhesion and lamellipodial protrusion dynamics is expected to play an important role in the adhesion-based modulation of directional persistence. Lamellipodial protrusion in migrating cells occurs via repeating waves of actin polymerization and membrane ruffling (Bailly et al., 1998b; Bear et al., 2002; Hinz et al., 1999). It has been reported that these waves of membrane extension do not require adhesion to occur, but that cell-substratum adhesion conditions the shape and stability of the protrusions (Bailly et al., 1998b). Importantly, although the extension and retraction of an individual lamellipodial wave occurs on the order of seconds to minutes (Bear et al., 2002; Hinz et al., 1999), the random directional behavior of a cell manifests at much longer timescales. Thus, a crucial part of understanding adhesion-mediated directional persistence is deconstructing whether adhesion-mediated variations in short-timescale spatial and temporal lamellipodial dynamics can control changes in long-timescale persistence time.

This work describes how variations in fibronectin-mediated cell-substratum adhesion affect both the long-timescale directional persistence and short-timescale membrane dynamics of migrating cells stimulated by the epidermal growth factor (EGF). The overexpression and ligand-induced activation of EGF receptor (EGFR), a prototypic receptor tyrosine kinase, correlates with increased invasiveness of

Submitted June 10, 2004, and accepted for publication November 9, 2004.

Address reprint requests to D. A. Lauffenburger, Biological Engineering Division, MIT, 56-341, 77 Massachusetts Ave., Cambridge, MA 02139. Tel.: 617-252-1629; Fax: 617-258-0204; E-mail: lauffen@mit.edu.

© 2005 by the Biophysical Society

0006-3495/05/02/1479/10 \$2.00

doi: 10.1529/biophysj.104.047365

tumors in vivo and increased migration of cell lines in vitro (Fontanini et al., 1995; Jorissen et al., 2003; McCrawley et al., 1997; Turner et al., 1996; Verbeek et al., 1998). EGF is also known to stimulate both actin polymerization and lamellipodial extension (Kurokawa et al., 2004; Nogami et al., 2003; Segall et al., 1996; Wells et al., 1999). Our model system consisted of Chinese hamster ovary (CHO) cells transfected with an EGFR-green fluorescent protein (GFP) fusion protein. Our choice of this system derived from the weakly adhesive nature of CHO cells. In weakly adherent cells, lamellipodial extension rate has been shown to limit EGF-mediated cell speed (Maheshwari et al., 1999). Also, unlike other weakly adherent cells like neutrophils and keratocytes that “glide” smoothly, CHO cells exhibit membrane extension steps that are relatively distinct from actual cell translocation. Together, these traits made CHO cells an attractive model system for studying the relationships between cell-substratum adhesion, lamellipodial protrusion, and the directional persistence of cell locomotion.

We find that EGF stimulation increases CHO cell motility, with the magnitude of increase correlating monotonically with increasing fibronectin (Fn) surface concentration. This increased motility results entirely from a Fn-dependent upregulation of persistence time in the presence of EGF, and actually conceals a mild decrease in cell speed. Both the overall increase in persistence due to EGF stimulation and the Fn-dependence of the magnitude of increase correlate with the temporal stability of individual waves of lamellipodial protrusion and retraction. Addition of soluble GRGDSP peptide, a competitive inhibitor of cell adhesion, decreases both persistence time and lamellipodial stability, indicating that directional migration is enhanced by adhesion-mediated protrusive stabilization. Our findings suggest that the short-timescale kinetics of adhesion complex formation may play a key role in modulating directional persistence over much longer timescales.

MATERIALS AND METHODS

Reagents and materials

Dulbecco's modified Eagle's medium, OptiMEM, fetal bovine serum (FBS), L-glutamine, sodium pyruvate, nonessential amino acids, penicillin, streptomycin, geneticin/G418 sulfate, HEPES, trypsin, versene (EDTA solution not containing any proteases), and phosphate-buffered saline (PBS) were purchased from Life Technologies (Carlsbad, CA). Bovine serum albumin (BSA), human Fn, and recombinant human EGF were purchased from Sigma Chemical (St. Louis, MO). Tissue culture flasks were purchased from Corning (Acton, MA). Unless noted, all other reagents were purchased from Sigma.

Construction of EGFR-pEGFP-N1 expression plasmid

The EGFR cDNA in pRC CMV2 vector (Invitrogen, Carlsbad, CA) was kindly provided by Dr. Steven Wiley (Pacific Northwest National Laboratories, Richland, WA). Using *Xba*I and *Hind*III sites, the cDNA was excised and cloned into pCR 2.1 TOPO (Invitrogen), which was used as

an intermediate cloning vector. The 5' terminus of the cDNA was then polymerase chain reaction-amplified using the following sets of primers:

Sense: 5'-GAGACCCACACTACCAG-3'

Antisense: 5'-TAAAGCTTAAGTGCTCCAATAAATTCAGT-3'.

The antisense primer was designed to introduce a *Hind*III site (underlined) and disrupt the stop codon.

The polymerase chain reaction product was ligated into pCR 2.1 TOPO, subsequently digested with *Hinc*II/*Hind*III, and cloned into the same sites on the full length EGFR cDNA in pCR2.1 TOPO. The full length EGFR cDNA (with the stop codon disrupted) was then removed from pCR2.1 TOPO using *Xba*I/*Hind*III sites and cloned into *Nhe*I/*Hind*III sites (*Xba*I and *Nhe*I produce compatible ends) on pEGFP-N1 (Clontech, Palo Alto, CA) for expression in mammalian cells. The completed plasmid was then sequenced to assure maintenance of the sequence of the original EGFR cDNA within the GFP fusion construct.

Creation of and maintenance of cell lines

Lipofectamine (Life Technologies) was used to transfect CHO K1 cells with EGFR-GFP according to manufacturer's protocols. After transfection, the cells were grown in selection medium (growth medium containing 1 mg/ml G418; see below) for 10 days. Two rounds of fluorescence-activated cell sorting were used to isolate a population of cells having GFP fluorescence ~20-fold above control. Transfected cells were grown in high-glucose Dulbecco's modified Eagle's medium containing 10% FBS (v/v), 2 mM glutamine, 1 mM sodium pyruvate, 1 mM nonessential amino acids, 100 U/ml penicillin, and 100 µg/ml streptomycin, along with 500 µg/ml G418 for plasmid expression maintenance. All cells were passaged at subconfluence and maintained in a 5% CO₂ environment. Maintenance of plasmid expression level with successive passages was tested via a fluorescence-activated cell sorter, with average expression level of EGFR-GFP decreasing by ~1/3 after 12 passages (data not shown). Only cells within this range of passage number were used for experiments; we were unable to ascertain any variation in results within this amount of drift in receptor expression level.

Preparation of surfaces for experiments

Glass-bottomed migration culture dishes (Biopetechs, Butler, PA) were sterilized using ultraviolet light and incubated overnight at 4°C with 1–30 µg/ml Fn dissolved in 0.5 ml PBS. The Fn solution was aspirated and the dishes rinsed twice with PBS. Dishes were then incubated for 1 h at 37°C with 0.5 ml 1% BSA in PBS. The BSA solution was aspirated and the dishes rinsed twice with PBS. All prepared dishes were stored under PBS at 37°C until ready for use (<30 min in all cases).

Cell pretreatment for experiments

While in midexponential growth, cells were serum-starved for 18 h in medium substituting 2 mg/ml BSA for the FBS in growth medium. Starved cells were lifted from culture plates using protease-devoid versene, then pelleted and resuspended for 1 h in serum-free medium buffered with 15 mM HEPES rather than sodium bicarbonate. Cell suspension was conducted to eliminate any residual adhesion-based intracellular signaling of starved cells. After cell suspension, cells were pelleted and resuspended in assay medium consisting of OptiMEM supplemented with penicillin (100 U/ml) and streptomycin (100 µg/ml), as well as 25 nM EGF and GRGDSP/GRADSP peptide (Calbiochem, San Diego, CA) as appropriate.

Long-timescale migration assay

Cell motility data was generated using a single-cell time-lapse videomicroscopy system consisting of an inverted microscope with 10×-magnification differential interference contrast objective (Carl Zeiss Microimaging,

Thornwood, NY); motorized xy -stage, z -focus drive, and shutter (Ludl Electronic Products, Hawthorne, NY); charge-coupled device camera (Hamamatsu Photonics, Bridgewater, NJ); and automated data acquisition software (Improvision, Lexington, MA). For maintenance of cell viability, a temperature-control system was used that electrically heats the underside of the migration assay dish (Biopetech). Additionally, a metal lid with glass aperture was placed on top of the assay dish such that no air pocket remained above the medium.

Cells suspended in assay medium (17,500 total per experiment) were plated onto Fn-coated assay dishes and allowed to adhere for 3 h for steady-state cell translocation behavior to develop (data not shown). Twenty separate fields containing 80–100 total cells were digitally imaged every 15 min for 6 h. Cell outlines and xy -centroids were determined using commercial image processing software (DIAS, Solltech, Oakdale, IA). Only cells that did not divide, touch other cells, or leave the image field during the experiment were used for data analysis; this restriction eliminated up to 25% of the cells initially tracked but did not affect any experimental conclusions.

Speed, persistence, and cell area data analysis

Mean-squared displacements for the centroid path of each cell were calculated using the method of nonoverlapping intervals (Dickinson and Tranquillo, 1993a). In this method, a cell tracked for N sequential positions with constant time interval Δt has mean-squared displacement for time interval $t_i = i \Delta t$ of

$$\langle d \cdot d(t_i) \rangle = \frac{1}{n_i} \sum_{j=1}^{n_i} d \cdot d_{(1+i(j-1))\Delta t \rightarrow (1+ij)\Delta t},$$

$$i = [1, 2, \dots, N-1]$$

$$n_i = \text{floor} \left\{ \frac{N-1}{i} \right\}$$

where *floor* represents the largest integer less than or equal to the bracketed quotient. Each cell's speed was determined by dividing the root mean-square displacement when $i = 1$ by the tracking interval $\Delta t = 15$ min. Each cell's persistence time was fit using nonlinear least-squares regression by inserting its speed into a persistent random walk model for cell migration (Dunn, 1983; Othmer et al., 1988):

$$\langle d \cdot d(t_i) \rangle = 2S^2P[t_i - P(1 - \exp\{-t_i/P\})].$$

Individual cell speeds and persistence times from each experiment were averaged to obtain a single experiment's parameter means and the associated standard errors. Each experiment was repeated at least three times; the reported S and P data are nonweighted averages across these separate experiments. Associated error bars represent ± 2 SE and were derived using standard propagation of error techniques. Analysis of variance (ANOVA) results were derived using the experimental means for S and P .

Individual cell areas were obtained using the cell outline determination described above. Average experimental cell areas were derived in a similar manner as in the speed and persistence analysis; associated error bars represent ± 2 SE. All computational routines were implemented in MATLAB 5.3 (The MathWorks, Natick, MA).

Kymography

To generate kymographs, cells were treated and plated as in the long-timescale migration experiments. Time-lapse movies were obtained using a 40 \times -magnification phase-contrast objective; each movie consisted of 2–3 cells observed over 25 min with an image capture interval of 5 s. Kymographs were produced using Metamorph software (Universal Imaging, Downingtown, PA). Briefly, a one-pixel-wide line was drawn perpendicular to the cell membrane at the location of an active protrusion event; image

information along this line was compiled sequentially from each movie frame and pasted into a composite image. The resulting image records membrane dynamics at a single region of the cell perimeter. Kymographs were analyzed by drawing straight lines from the beginning of each protrusion event to its peak, neglecting protrusion heights of < 3 pixels (0.5 μm). The slopes of these lines represent protrusion velocity, and the x axis projection distances of these lines represent protrusion stability (Bear et al., 2002; Hinz et al., 1999). Reported data ± 2 SE represent the mean of two independent experiments per condition with 15–20 cells and 150–200 individual protrusion events per experiment.

RESULTS

EGF increases cell motility in CHO-EGFR cells in a manner dependent on Fn coating concentration

EGF receptor expression and ligation stimulate migration in many cell lines, including keratinocytes, epithelial cells, and fibroblasts (McCrawley et al., 1997; Verbeek et al., 1998; Wells et al., 1998). Previous studies have demonstrated that EGF activates actin polymerization and lamellipodial protrusion (Bailly et al., 1998b; Segall et al., 1996), and that at low levels of adhesiveness, lamellipodial protrusion rate limits overall EGF-stimulated motility (Maheshwari et al., 1999; Ware et al., 1998). Taking these facts together, we elected to use CHO cells for our motility experiments because they are weakly adhesive yet exhibit easily observable membrane protrusions.

However, as CHO cells do not express endogenous EGFR, we first examined whether exogenous EGFR expression and subsequent EGF stimulation influenced CHO cell motility. We created a plasmid vector linking GFP to the C-terminus of EGFR and stably transfected it in CHO cells. Previous studies have established that fusion of GFP to the C-terminus of EGFR does not affect EGFR function as judged by rates of receptor downregulation and internalization (Carter and Sorkin, 1998). Time-lapse single-cell videomicroscopy experiments were then used to track the migration of these transfected cells on glass surfaces adsorbed with the extracellular matrix protein Fn, which binds to $\alpha_5\beta_1$ integrins expressed by the CHO cells.

Using wind-rose plots, Fig. 1 depicts the change in individual CHO cell tracks resulting from EGFR-GFP transfection, varying Fn coating concentration, and the presence and absence of EGF. Initial experiments demonstrated that, as expected, the migration of untransfected CHO K1 cells was unchanged in response to EGF (Fig. 1, A and B). In contrast, transfected CHO-EGFR cells demonstrated upregulated migration upon stimulation by EGF (Fig. 1, C–F). To better understand the nature of the EGF-dependent response, we assessed the role of cell-substratum adhesion in modulating EGF-dependent CHO-EGFR cell migration by using a broad range of Fn coating concentrations (1, 3, 10, and 30 $\mu\text{g/ml}$). To more clearly reveal the results, we have plotted cell tracks from the two extremes of Fn coating concentration (1 and 30 $\mu\text{g/ml}$). EGF stimulation augmented cell motility at all Fn coating concentrations, with the level of

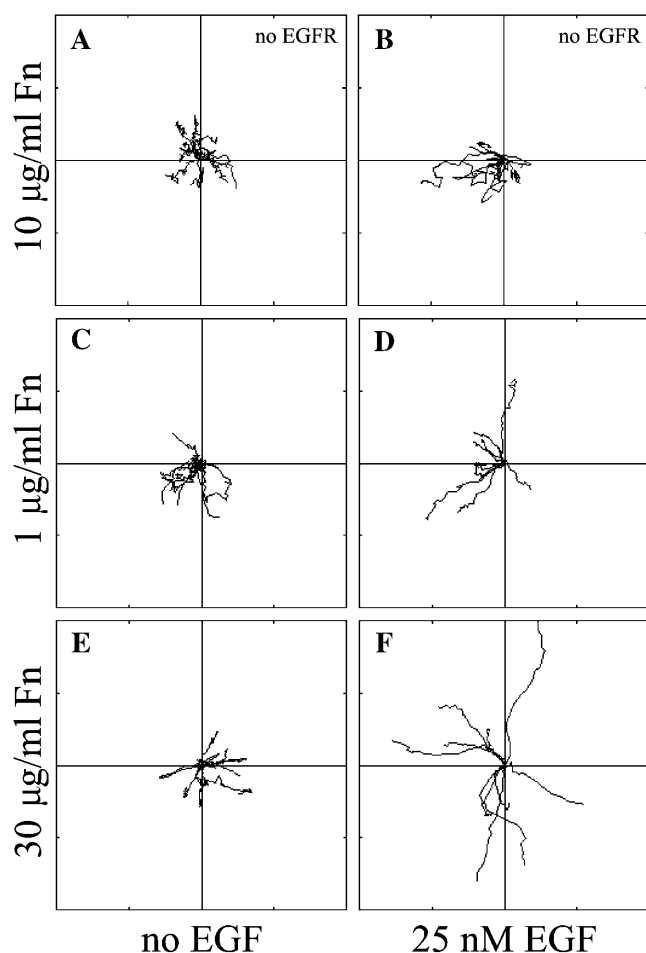


FIGURE 1 Migration behavior of EGFR-transfected CHO cells is affected by Fn and EGF. Time-lapse videomicroscopy was used to capture the motility responses of individual CHO K1 and CHO-EGFR cells. (A and B) Without EGFR-GFP transfection, EGF does not affect the migratory response of CHO K1 cells; (C–F) Transfected CHO-EGFR cells respond to EGF by upregulating their migration in a Fn-dependent manner. Digital images were taken every 15 min for a total of 6 h per experiment. Each wind-rose plot shows centroid tracks from 10 representative cells in a typical experiment, with the initial position of each track superimposed at 0,0 for clarity. Distance between hatch marks on both axes is 50 μ m.

EGF-mediated motility rising as Fn coating concentration increased (Fig. 1, D and F). In the absence of EGF, cell motility showed no qualitative dependence on Fn concentration (Fig. 1, C and E). Taking these results together, the CHO-EGFR cell system exhibits the expected upregulation of migration in response to EGF stimulation, but the migration response is a complex output resulting from variations in Fn coating concentration and EGF stimulation.

Fn and EGF effects on speed and persistence time

The paths of individual migrating cells can be described using a persistent random walk model characterized by two phenomenological parameters: cell speed (S) and persistence

time (P) (Dunn, 1983; Gail and Boone, 1970; Othmer et al., 1988). Use of these parameters permits a quantitative analysis of the qualitative differences in migration behavior observed in the wind-rose diagrams. By fitting cell path mean-squared displacement data to the persistent random walk model, we obtained S and P data characterizing CHO-EGFR migration responses to Fn and EGF (Fig. 2).

Consistent with the results of Fig. 1, neither the speed nor the persistence of untransfected CHO K1 cells varied with addition of EGF (Fig. 2, A and B). Moreover, the transfection of EGFR-GFP did not alter the speed or persistence of CHO cells in the absence of EGF. However, transfected CHO-EGFR cells demonstrated differences in speed and persistence upon EGF ligation. In both the absence and presence of EGF, we found that the average speed of CHO-EGFR cells was roughly constant across all tested Fn coating concentrations (Fig. 2 C). In the absence of EGF, S was $\sim 16 \mu\text{m/h}$; in the presence of EGF we observed an unexpected but consistent decrease in S to $\sim 13 \mu\text{m/h}$. Directional persistence of CHO-EGFR cells in the absence of EGF was low and showed a weak, statistically insignificant increase from ~ 11 to ~ 15 min as Fn coating concentration was increased from 1 $\mu\text{g/ml}$ to 30 $\mu\text{g/ml}$ (Fig. 2 D). EGF addition increased P at all Fn levels. Moreover, P in the presence of EGF showed a strong dependence on Fn concentration, rising from ~ 22 min at 1 $\mu\text{g/ml}$ to ~ 43 min at 30 $\mu\text{g/ml}$. We conclude that our qualitative observations showing a Fn-dependent increase in EGF-stimulated cell migration (Fig. 1) result from increases in directional persistence time but not an increase in cell speed.

Changes in the temporal stability of lamellipodial protrusions correlate to variations in cell persistence time

Previous investigations of the combined effects of EGF stimulation and extracellular matrix surface density on fibroblast migration indicate that EGF upregulates cell speed at medium and high matrix surface densities, but reduces speed under conditions of weak cell-substratum adhesion (Maheshwari et al., 1999; Ware et al., 1998). We reasoned that our observed reduction in cell speed upon EGF stimulation indicated that the CHO-EGFR cells were weakly adhesive across all tested Fn coating concentrations.

The translocation speed of weakly adhesive cells is limited by the rate of lamellipodial protrusion (DiMilla et al., 1991; Lauffenburger, 1989; Maheshwari et al., 1999; Ware et al., 1998). In an analogous fashion, we hypothesized that the stability of membrane protrusions was related to both the EGF-dependent upregulation of directional persistence and the observed linear relationship between EGF-mediated directional persistence and Fn coating concentration. This hypothesis accorded with previous evidence suggesting that although the initial protrusion of EGF-stimulated lamellipods does not require cell-substratum adhesion, protrusions

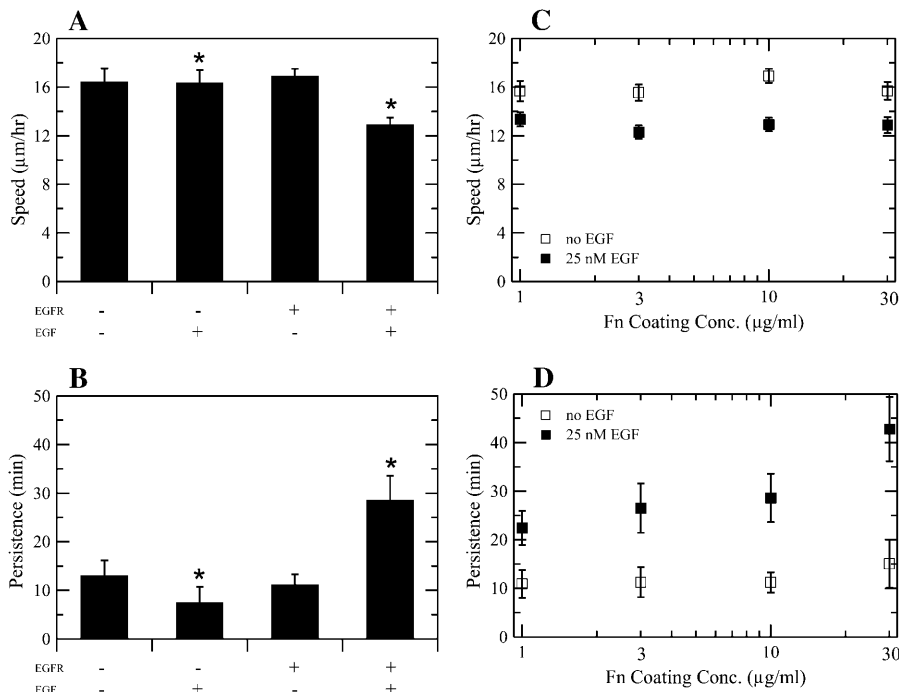


FIGURE 2 Effects of EGF and Fn on speed and persistence for migrating CHO-EGFR cells. Transfection of EGFR-GFP into CHO K1 cells alters cell speed (A) and persistence (B) in the presence, but not the absence, of EGF. Data in A and B were obtained using a 10 $\mu\text{g/ml}$ Fn coating concentration. Asterisks denote inequality at 95% confidence for key comparison. (C) EGF stimulation, but not Fn coating concentration, modulates CHO-EGFR speed. Single-factor ANOVA: $p = 0.54$ (S , -EGF), $p = 0.90$ (S , +EGF). (D) Persistence time increases with Fn coating concentration in the presence of EGF. ANOVA: $p = 0.88$ (P , -EGF), $p = 0.03$ (P , +EGF). To derive the speed of a single cell, total cell path length was divided by the total time of observation. Single cell persistence times were derived from non-linear least-squares regression using individual cell speed and root mean-square displacement data as inputs. Reported S and P data represent the mean \pm 2 SE for three experiments per condition, with 80–100 cells per experiment.

retract quickly when extended over nonadhesive substrates (Bailly et al., 1998b). To test the hypothesis, we used kymography to analyze lamellipodial dynamics (Hinze et al., 1999). Kymographs are composite time-space images of membrane movement at a single point of an actively protruding lamellipod, created by extracting image information from a defined line region in each image of a time-lapse movie and pasting them side-by-side. Whereas cell translocation experiments captured one movie frame every 15 min, kymography studies captured one movie frame every 5 s. As a result of this high temporal resolution, we were able to observe the local dynamics of individual lamellipodial protrusion and retraction cycles on a much shorter timescale than that required for net CHO-EGFR cell translocation, separating the effects of two related, but not equivalent, aspects of cell motility.

Fig. 3 contains two representative kymographs showing the qualitative difference in EGF-stimulated membrane dynamics between 1 $\mu\text{g/ml}$ and 30 $\mu\text{g/ml}$ Fn coating concentration. Lamellipodia at the lower amount of Fn exhibited small, quickly oscillating waves of protrusion and retraction of membrane; lamellipodia at the higher amount exhibited smoother, more sustained protrusion with less frequent retractions. To quantify this observed difference in lamellipodial behavior, we analyzed how the velocity and stability of individual lamellipodial protrusion waves varied with Fn coating concentration. Protrusion velocity represents the average spatial rate of actin polymerization from the beginning of a single protrusion wave to its peak, whereas protrusion stability measures the time spanned by that wave. As shown in Fig. 4 A, protrusion velocity remained constant

with variations in EGF stimulation and Fn concentration, at $\sim 2.2 \mu\text{m/min}$ (ANOVA $p = 0.86$). In contrast, Fig. 4 B shows that the addition of EGF increased the average stability of individual membrane protrusion waves from 0.55 min to 0.72 min at 30 $\mu\text{g/ml}$ Fn ($p = 0.04$). In addition, the temporal stability of EGF-stimulated protrusion waves increased monotonically from 0.44 min at 1 $\mu\text{g/ml}$ Fn coating concentration to 0.72 min at 30 $\mu\text{g/ml}$ Fn (ANOVA $p = 0.03$). Comparison with Fig. 2 B indicates that these

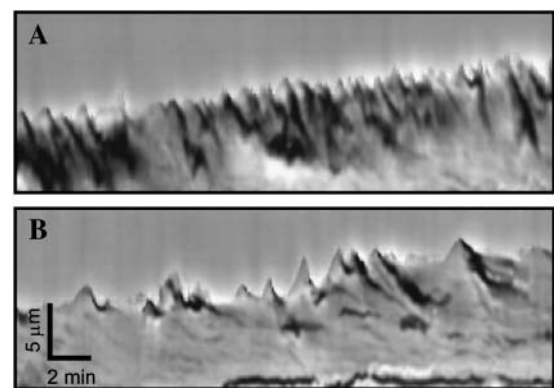


FIGURE 3 Lamellipodial membrane dynamics of CHO-EGFR cells. Representative short-timescale kymographs from time-lapse movies of CHO-EGFR cells stimulated with EGF and migrating on 1 $\mu\text{g/ml}$ (A) and 30 $\mu\text{g/ml}$ (B) Fn. Kymographs depict variations in lamellipodial activity along a one-pixel-wide line drawn perpendicularly to the cell membrane in sequential phase contrast images. Ascending contours show lamellipodial protrusion, whereas descending contours show lamellipodial retraction. Dark regions indicate membrane ruffling.

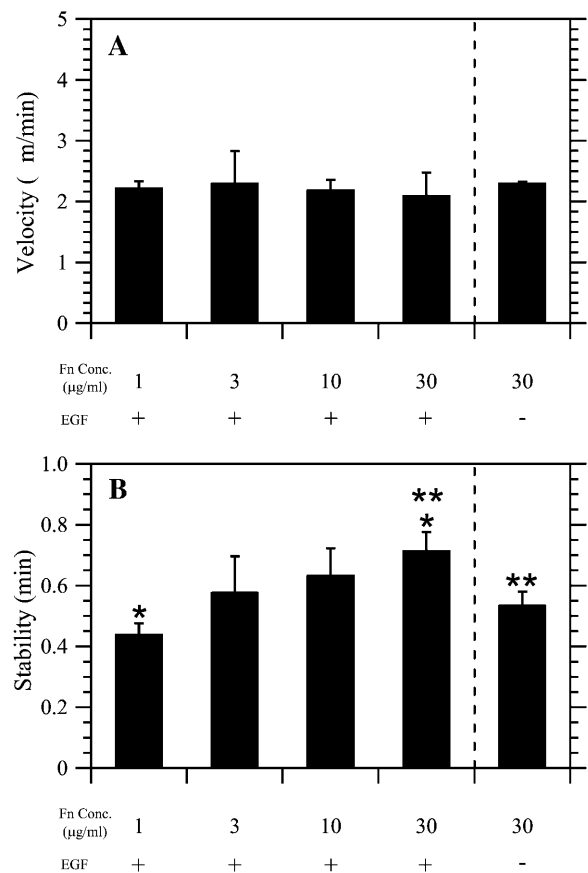


FIGURE 4 Lamellipodial stability correlates with directional persistence in CHO-EGFR migration. (A) Fn coating concentration does not affect the average velocity of membrane protrusion. The average slope of ascending kymograph membrane waves defines protrusion velocity. ANOVA: $p = 0.86$. (B) Protrusion stability increases with Fn concentration in the presence of EGF. Stability represents the time elapsed between the beginning of a single protrusion wave and its spatial peak. Nonoverlapping 95% confidence intervals are indicated by asterisks. ANOVA: $p = 0.03$.

results occur in parallel with EGF- and Fn-dependent changes in P . Hence, a correlation exists between the short-timescale stability of lamellipodial protrusions and long-timescale directional persistence of translocating CHO-EGFR cells.

Soluble RGD peptide reduces both long-timescale directional persistence and short-timescale protrusion stability

The Fn-based correlation in Fig. 4 B implies that variations in cell-substratum adhesion strength can affect the long-timescale directional persistence of cell paths through modulation of the stability of short-timescale local membrane protrusion events. To gain better insight into this possibility, we performed both cell translocation and membrane dynamics studies in the presence of soluble GRGDSP peptide. Synthetic peptides containing the RGD

sequence are competitive inhibitors of Fn binding to $\alpha_5\beta_1$ integrins, and have been shown previously to inhibit cell adhesion and migration (Fujii et al., 1998; Libotte et al., 2001; Shimizu et al., 1997). To confirm the inhibitory effect of the peptide on CHO-EGFR adhesion, we calculated average cell areas for cells migrating in the presence of EGF and GRGDSP peptide. Cell area increased in parallel with increasing Fn coating concentrations (Fig. 5). This Fn-dependent effect on overall cell area was counterbalanced by a dose-dependent decrease of cell area upon addition of GRGDSP, confirming that addition of soluble peptide inhibited cell adhesion. To study the migratory response of EGF-stimulated cells to GRGDSP peptide, 30 μ g/ml Fn coating concentration was chosen as the condition giving the highest directional persistence time and most stable membrane protrusion events. We found that the addition of 100 and 300 μ M GRGDSP decreased the motility of CHO-EGFR cells in a dose-dependent fashion as demonstrated by wind-rose plots (Fig. 6 A). Quantification of this GRGDSP-dependent inhibition of cell motility revealed that speed was unaffected (Fig. 6 B), while the persistence of the CHO-EGFR cells decreased to 33 and 29 min, respectively, from a baseline of 43 min (Fig. 6 C). Addition of 300 μ M GRADSP control peptide had no effect on S or P . Similarly to the effects on speed and persistence, 300 μ M GRGDSP peptide reduced the stability of lamellipodial protrusion events in a statistically significant manner while not affecting lamellipodial velocity (Fig. 6 D and data not shown). In contrast, the addition of control GRADSP peptide had no effect on lamellipodial protrusion stability. These results provide further evidence that adhesion strength modulates persistence time, and show that long-timescale directional migration is enhanced by adhesion-mediated stabilization of short-timescale lamellipodial protrusions.

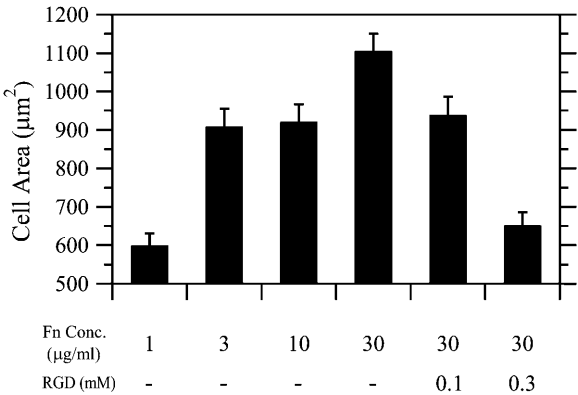


FIGURE 5 Soluble RGD peptide inhibits cell adhesion. The average area of CHO-EGFR cells migrating in the presence of EGF was determined for all Fn coating concentrations; cell adhesion as described by cell area increased in parallel with Fn. Addition of peptide inhibitor abrogated this Fn-dependent effect on adhesion in a dose-dependent fashion.

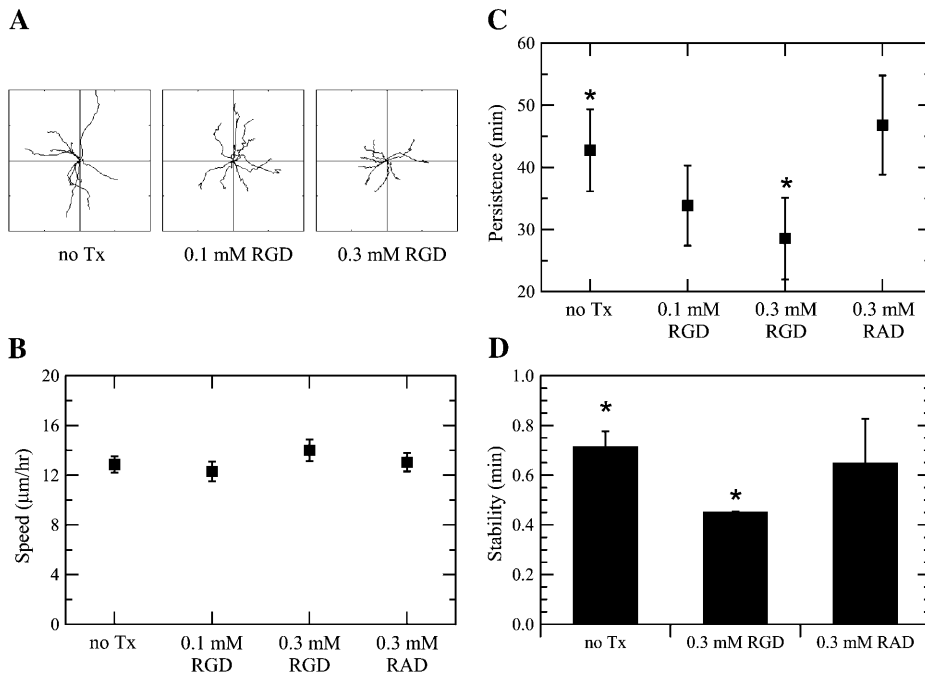


FIGURE 6 RGD peptide reduces both long-timescale directional persistence and short-timescale protrusion stability. (A) Wind-rose plots for migration experiments of CHO-EGFR cells plated on 30 $\mu\text{g/ml}$ Fn in the presence of EGF and varying amounts of GRGDSP, a soluble competitive inhibitor of Fn binding to $\alpha_5\beta_1$ integrins. Distance between hatch marks on both axes is 50 μm . (B) Cell speeds and (C) persistence times for the RGD migration experiments. Speed and persistence were derived as in Fig. 2. ANOVA: $p = 0.71$ for RGD-dependent cell speed, $p = 0.002$ for RGD-dependent persistence. Nonoverlapping 95% confidence intervals are indicated by asterisks. (D) Kymography was performed on CHO-EGFR cells plated on 30 $\mu\text{g/ml}$ Fn in the presence of EGF and either GRGDSP or control GRADSP peptide. Nonoverlapping 95% confidence intervals are indicated by asterisks ($p = 0.01$).

DISCUSSION

Individual cell migration exhibits sustained locomotion in the direction of the leading lamellipod over short periods of time and random changing of the directional orientation of lamellipodial protrusion and migration over longer time-scales (Dunn, 1983; Maheshwari and Lauffenburger, 1998). This persistent random walk is characterized by both speed and directional persistence time. But though the role of cell-substratum adhesion in modulating S has been characterized extensively (DiMilla et al., 1993; Goodman et al., 1989; Maheshwari et al., 1999; Palecek et al., 1997), it is not well understood how variations in cell-substratum adhesion modulate P . In this study, we have described how varying the surface coating concentration of Fn substrate modulates P for EGF receptor-transfected CHO cells, and explored how adhesion-dependent changes in lamellipodial protrusion dynamics might explain our results. Our major findings are: a), EGF stimulation increases P across all Fn concentrations but actually reduces S ; b), EGF also increases the temporal stability, but not the velocity, of individual lamellipodial protrusion waves; c), in the presence of EGF, both P and protrusion stability increase with higher Fn coating concentration; and d), in the presence of EGF, the addition of GRGDSP peptide, a soluble competitive inhibitor of cell-substratum binding, reduces both P and the stability of lamellipodia.

Stochastic kinetic fluctuations in adhesion receptor binding and intracellular transport have been proposed as a mechanistic basis for directional persistence in uniform adhesive environments (Dickinson and Tranquillo, 1993b). This model links these short-timescale fluctuations to

variations in spatiotemporal forces that affect the speed and direction of cell migration on longer timescales. The model predicts an inverted biphasic dependence of persistence time to cell-substratum adhesion strength; however, previous studies of the relationship between substratum coating density and persistence have not confirmed this prediction (DiMilla et al., 1993; Ware et al., 1998). Our observation of a monotonic rather than inverted biphasic curve relating EGF-dependent directional persistence and Fn coating concentration (Fig. 2 B) could be reconciled with the stochastic model by postulating a cell type-dependent inability to experimentally access a wide enough dynamic range of adhesion strength. However, a linear correlation between increasing Fn coating concentration and increasing EGF-mediated persistence is consistent with the Dickinson persistence model only if our CHO cells are migrating under conditions of high adhesiveness (Dickinson and Tranquillo, 1993b).

In contrast, the CHO-EGFR cells appear to be only weakly adhesive under all the conditions studied. Fn coating concentrations of $<1 \mu\text{g/ml}$ were insufficient for the adherence and spreading of cells (data not shown). Furthermore, the cells exhibited decreased cell speed upon EGF stimulation (Fig. 2 C), and a previous study of the combined role of EGF and Fn in fibroblast motility has demonstrated that EGF increases S at medium and high levels of cell adhesion while decreasing S at low levels (Maheshwari et al., 1999). This decrease in S at low adhesiveness is caused by an EGF-dependent reduction in cell-substratum adhesivity (Maheshwari et al., 1999; Xie et al., 1998). We also tested the role of M-calpain, the cytoskeletal protease that mediates the de-adhesive effect of

EGF (Glading et al., 2002), in modulating CHO-EGFR cell speed. Pharmacologic inhibition of M-calpain activity did not reduce S (data not shown), a result expected for weakly adherent, but not strongly adherent cells (Glading et al., 2002; Huttenlocher et al., 1997).

In addition to the EGF-mediated decrease in S , another interesting aspect of our results is that CHO-EGFR speed in the presence of EGF is independent of Fn coating concentration, whereas persistence shows substantial Fn-dependent variation (Fig. 2, *C* and *D*). One possible explanation involves separating the effects of EGFR signaling on adhesion into separate modules regulating overall adhesion strength and front-rear adhesive asymmetry. These modules would in turn control S and P , respectively. Mathematical modeling suggests that variations in S result from changes in overall adhesion strength relative to the amount of contractile force generated in a cell (DiMilla et al., 1991). The CHO-EGFR cells presumably maintain these in roughly constant balance across all the Fn concentrations studied, with a change in speed only occurring due to the de-adhesive effect of EGF (Maheshwari et al., 1999). However, in concert with its overall de-adhesive effect, EGF also increases front-rear adhesive asymmetry by accentuating morphological polarization (Wells et al., 1999) and eliciting the creation of new focal complexes at the cell front (Bailly et al., 1998a). Greater adhesive asymmetry could be expected to reinforce a cell's ability to maintain its migration in a constant direction and thus account for the increase in CHO-EGFR persistence when stimulated by exogenous EGF. Interestingly, that the stability of lamellipodial protrusion events also increases upon addition of EGF (Fig. 4 *B*) indirectly supports the idea that EGF actually increases adhesion at the front of cells. Moreover, that increasing amounts of surface Fn correlate with increasing EGF-stimulated persistence suggests that increased adhesive asymmetry downstream of EGF receptor signaling is merely permissive for P , with the level of cell-substratum adhesion actually controlling the effective level of EGFR signaling.

The rate of actin polymerization in membrane protrusions and ruffles has been shown to be independent of adhesion (Bailly et al., 1998b; Felder and Elson, 1990). Our observations are consistent with this fact in that EGF-stimulated protrusion velocity ($\sim 2.2 \mu\text{m}/\text{min}$) does not depend on Fn coating concentration. In contrast, that EGF-stimulated lamellipodial stability increases with Fn concentration (Fig. 4 *B*), and that P and lamellipodial stability are reduced concurrently by GRDGSP peptide (Fig. 6, *C* and *D*), both imply that cell-substratum adhesion mediates the connection between short-timescale lamellipodial protrusion and long-timescale directional persistence in our experiments. Our findings recall a previous report correlating lamellipodial protrusion rate with net cell translocation speed under weakly adhesive conditions (Maheshwari et al., 1999); both S and P regulate the amount of net cell motility. However, Maheshwari et al. measured lamellipodial exten-

sion using the same long-timescale temporal rate of image capture as their experiments studying net cell translocation. As a result, their reported lamellipodial extension rates would intrinsically be related to S . On the basis of our results, we suggest that the lamellipodial extension rates of Maheshwari et al. might conceal an analogous relationship between short-timescale protrusion stability and long-timescale cell speed. Others have reported such a relationship, though not in the context of cell-substratum adhesion (Bear et al., 2002).

Our observations of Fn- and GRGDSP-dependent variations in protrusion stability likely derive from mass action kinetics, in that greater amounts of Fn surface coating lead to more efficient short-timescale binding of CHO $\alpha_5\beta_1$ integrins and the formation of more protrusion-stabilizing focal complexes near the leading edge. In turn, the directional persistence of migration could be considered a long-timescale temporal integration of the net amount of adhesion formation on the much shorter timescale of individual lamellipodial protrusion waves. Cells forming new adhesions more slowly would be more likely to retract a lamellipod and attempt to migrate in a new direction. Consistent with this idea is the work of Bailly et al. (1998b) demonstrating that EGF-stimulated actin polymerization and membrane extension do not require adhesion to occur, but that a lack of cell-substratum adhesion reduces the stability of protrusions.

Overall, our studies of Fn- and GRGDSP-dependent variations in protrusion stability point toward the regulated assembly of adhesion complexes as a locus of molecular control of directionality in motility. What proteins might play a key role as molecular switches linking adhesion formation to directional persistence? Recent studies suggest that vinculin is a necessary focal complex protein for transmitting cytoskeletal traction force and linking membrane protrusion to matrix adhesion (DeMali et al., 2002; Galbraith et al., 2002). The spatially or temporally regulated addition of vinculin or other specific proteins to lamellipodial adhesions could serve as a link coordinating short-timescale actin polymerization dynamics with directed cell translocation that occurs over longer timescales. Another recent report indicates that myosin light-chain kinase (MLCK) plays a role in stabilizing lamellipodial protrusions (Totsukawa et al., 2004). Totsukawa and colleagues found that in MLCK-inhibited fibroblasts, nascent adhesions at the tips of lamellipodia did not mature into larger adhesive structures; moreover, the protrusions of these MLCK-inhibited cells were less stable and retracted more frequently. Interestingly, they report wind-rose plots indicating that MLCK inhibition substantially reduces cell motility by increasing the directional tortuosity of cell paths. Given the well-established role of MLCK-promoted contractility in focal adhesion assembly and the modulation of both cell adhesion and cell motility (Brahmbhatt and Klemke, 2003; Burridge and Chrzanowski-Wodnicka, 1996; Klemke et al.,

1997), it is plausible that lamellipodial MLCK activity, like vinculin recruitment, could act as a molecular switch modulating adhesion-mediated directional persistence.

It is interesting to speculate that underlying the results of this study there exists a monotonic relationship between directional persistence, protrusion stability, and the quantitative lamellipodial recruitment and activation of specific adhesion-related proteins such as vinculin or MLCK. To our knowledge, this hypothesis has not been tested rigorously. We note that the quantity of recruitment need not depend solely on the amount of extracellular adhesion substrate. Presumably such recruitment would also occur downstream of both integrin- and growth factor-mediated signaling pathways known to potentiate cell polarization and directional cell migration such as PLC γ , PI3K, Cdc42, and Rac (Kiosses et al., 2001; Ridley, 2001; Weiner, 2002; Wells et al., 1999).

The authors thank Mykola Kovalenko for creating the EGFR-GFP construct, Alia Burton for assistance in kymograph analysis, and Alan Wells, Frank Gertler, and Lily Koo for helpful discussions.

Funding for this work was provided by National Cancer Institute grant CA88865 to D.A.L.

REFERENCES

- Bailly, M., J. S. Condeelis, and J. E. Segall. 1998a. Chemoattractant-induced lamellipod extension. *Microsc. Res. Tech.* 43:433–443.
- Bailly, M., L. Yan, G. M. Whitesides, J. S. Condeelis, and J. E. Segall. 1998b. Regulation of protrusion shape and adhesion to the substratum during chemotactic responses of mammalian carcinoma cells. *Exp. Cell Res.* 241:285–299.
- Bear, J. E., T. M. Svitkina, M. Krause, D. A. Schafer, J. J. Loureiro, G. A. Strasser, I. V. Maly, O. Y. Chaga, J. A. Cooper, G. G. Borisy, and F. B. Gertler. 2002. Antagonism between Ena/VASP proteins and actin filament capping regulates fibroblast motility. *Cell*. 109:509–521.
- Brahmbhatt, A. A., and R. L. Klemke. 2003. ERK and RhoA differentially regulate pseudopodia growth and retraction during chemotaxis. *J. Biol. Chem.* 278:13016–13025.
- Burridge, K., and M. Chrzanowski-Wodnicka. 1996. Focal adhesions, contractility, and signaling. *Annu. Rev. Cell Dev. Biol.* 12:463–519.
- Carter, R. E., and M. Sorkin. 1998. Endocytosis of functional epidermal growth factor receptor-green fluorescent protein chimera. *J. Biol. Chem.* 273:35000–35007.
- DeMali, K. A., C. A. Barlow, and K. Burridge. 2002. Recruitment of the Arp2/3 complex to vinculin: coupling membrane protrusion to matrix adhesion. *J. Cell Biol.* 159:881–891.
- Dickinson, R. B., and R. T. Tranquillo. 1993a. Optimal estimation of cell movement indices from the statistical analysis of cell tracking data. *AIChE J.* 39:1995–2010.
- Dickinson, R. B., and R. T. Tranquillo. 1993b. A stochastic model for adhesion-mediated cell random motility and haptotaxis. *J. Math. Biol.* 31:563–600.
- DiMilla, P. A., K. Barbee, and D. A. Lauffenburger. 1991. Mathematical model for the effects of adhesion and mechanics on cell migration speed. *Biophys. J.* 60:15–37.
- DiMilla, P. A., J. A. Stone, J. A. Quinn, S. M. Albelda, and D. A. Lauffenburger. 1993. Maximal migration of human smooth muscle cells on fibronectin and Type IV collagen occurs at an intermediate attachment strength. *J. Cell Biol.* 122:729–737.
- Dunn, G. A. 1983. Characterizing a kinesis response; time averaged measures of cell speed and directional persistence. *Agents Actions*. 12(Suppl.):14–33.
- Felder, S., and E. L. Elson. 1990. Mechanics of fibroblast locomotion: quantitative analysis of forces and motions at the leading lamellas of fibroblasts. *J. Cell Biol.* 111:2513–2526.
- Fontanini, G., S. Vignati, D. Bigini, A. Mussi, H. Lucchi, C. A. Angeletti, R. Pingitore, S. Pepe, F. Basolo, and G. Bevilacqua. 1995. Epidermal growth factor receptor (EGFR) expression in non-small cell lung carcinomas correlates with metastatic involvement of hilar and mediastinal lymph nodes in the squamous subtype. *Eur. J. Cancer*. 31A:178–183.
- Fujii, H., N. Nishikawa, H. Komazawa, M. Suzuki, M. Kojima, I. Itoh, A. Obata, K. Ayukawa, I. Azuma, and I. Saiki. 1998. A new pseudo-peptide of Arg-Gly-Asp (RGD) with inhibitory effect on tumor metastasis and enzymatic degradation of extracellular matrix. *Clin. Exp. Metastasis*. 16:94–104.
- Gail, M. H., and C. W. Boone. 1970. The locomotion of mouse fibroblasts in tissue culture. *Biophys. J.* 10:980–993.
- Galbraith, C. G., K. M. Yamada, and M. P. Sheetz. 2002. The relationship between force and focal contact development. *J. Cell Biol.* 159:695–705.
- Glading, A., D. A. Lauffenburger, and A. Wells. 2002. Cutting to the chase: calpain proteases in cell motility. *Trends Cell Biol.* 12:46–54.
- Goodman, S. L., G. Risse, and K. von der Mark. 1989. The E8 subfragment of laminin promotes locomotion of myoblasts over extracellular matrix. *J. Cell Biol.* 109:799–809.
- Hart, J. 2002. Inflammation. 1: Its role in the healing of acute wounds. *J. Wound Care*. 11:205–209.
- Hinz, B., W. Alt, C. Johnen, V. Herzog, and H. W. Kaiser. 1999. Quantifying lamella dynamics of cultured cells by SAGED, a new computer-assisted motion analysis. *Exp. Cell Res.* 251:234–243.
- Huttenlocher, A., S. P. Palecek, Q. Lu, W. Zhang, R. L. Mellgren, D. A. Lauffenburger, M. H. Ginsberg, and A. F. Horwitz. 1997. Regulation of cell migration by the calcium-dependent protease calpain. *J. Biol. Chem.* 272:32719–32722.
- Jorissen, R. N., F. W. Walker, N. Pouliot, T. P. J. Garrett, C. W. Ward, and A. W. Burgess. 2003. Epidermal growth factor receptor: mechanisms of activation and signaling. *Exp. Cell Res.* 284:31–53.
- Kassis, J., D. A. Lauffenburger, T. Turner, and A. Wells. 2001. Tumor invasion as dysregulated cell motility. *Semin. Cancer Biol.* 11:105–117.
- Keller, R. 2002. Shaping the vertebrate body plan by polarized embryonic cell movements. *Science*. 298:1950–1954.
- Kiosses, W. B., S. J. Shattil, N. Pampori, and M. A. Schwartz. 2001. Rac recruits high-affinity integrin $\alpha_5\beta_3$ to lamellipodia in endothelial cell migration. *Nat. Cell Biol.* 3:316–320.
- Klemke, R. S., S. Kai, A. Giannini, P. Gallagher, P. de Lanerolle, and D. Cheresch. 1997. Regulation of cell motility by mitogen-activated protein kinase. *J. Cell Biol.* 137:481–492.
- Kraemer, R. 2000. Regulation of cell migration in atherosclerosis. *Curr. Atheroscler. Rep.* 2:445–452.
- Kurokawa, K., R. E. Itoh, H. Yoshizaki, Y. Ohba, T. Nakamura, and M. Matsuda. 2004. Coactivation of Rac1 and Cdc42 at lamellipodia and membrane ruffles induced by epidermal growth factor. *Mol. Biol. Cell*. 15:1003–1010.
- Lauffenburger, D. A. 1989. A simple model for the effects of receptor-mediated cell-substratum adhesion on cell migration. *Chem. Eng. Sci.* 44:1903–1914.
- Lauffenburger, D. A., and A. F. Horwitz. 1996. Cell migration: a physically integrated molecular process. *Cell*. 84:359–369.
- Libotte, T., H.-W. Kaiser, W. Alt, and T. Bretschneider. 2001. Polarity, protrusion-retraction dynamics and their interplay during keratinocyte cell migration. *Exp. Cell Res.* 270:129–137.
- Maheshwari, G., and D. A. Lauffenburger. 1998. Deconstructing (and reconstructing) cell migration. *Microsc. Res. Tech.* 43:358–368.

- Mareshwari, G., A. Wells, L. G. Griffith, and D. A. Lauffenburger. 1999. Biophysical integration of effects of epidermal growth factor and fibronectin on fibroblast migration. *Biophys. J.* 76:2814–2823.
- Martin, P. 1997. Wound healing: aiming for perfect regeneration. *Science*. 275:75–81.
- McCrawley, I. J., P. O'Brian, and L. G. Hudson. 1997. Overexpression of the epidermal growth factor receptor contributes to enhanced ligand-mediated motility in keratinocyte cell lines. *Endocrinology*. 138:121–127.
- Mitchison, T. J., and L. P. Cramer. 1996. Actin-based cell motility and cell locomotion. *Cell*. 84:371–379.
- Nogami, M., M. Yamazaki, H. Watanabe, Y. Okabayashi, Y. Kido, M. Kasuga, T. Sasaki, T. Maehama, and Y. Kanaho. 2003. Requirement of autophosphorylated tyrosine 992 of EGF receptor and its docking protein phospholipase C γ 1 for membrane ruffle formation. *FEBS Lett.* 536:71–76.
- Othmer, H. G., S. R. Dunbar, and W. Alt. 1988. Models of dispersal in biological systems. *J. Math. Biol.* 26:263–298.
- Palecek, S. E., J. C. Loftus, M. H. Ginsburg, D. A. Lauffenburger, and A. F. Horwitz. 1997. Integrin-ligand binding properties govern cell migration speed through cell-substratum adhesiveness. *Nature*. 385:537–540.
- Ridley, A. J. 2001. Rho GTPases and cell migration. *J. Cell Sci.* 114:2713–2722.
- Segall, J. E., S. Tyerach, L. Boselli, S. Masseling, J. Helft, A. Chan, J. Jones, and J. Condeelis. 1996. EGF stimulates lamellipod extension in metastatic mammary adenocarcinoma cells by an actin-dependent mechanism. *J. Cell Sci.* 14:61–72.
- Shimizu, M., K. Minakuchi, S. Kaji, and J. Koga. 1997. Chondrocyte migration to fibronectin, type I collagen, and type II collagen. *Cell Struct. Funct.* 22:309–315.
- Szekanecz, Z., and A. E. Koch. 2000. Endothelial cells and immune cell migration. *Arthritis Res.* 2:368–373.
- Totsukawa, G., Y. Wu, Y. Sasaki, D. J. Hartshorne, Y. Yamakita, S. Yamashiro, and F. Matsumura. 2004. Distinct roles of MLCK and ROCK in the regulation of membrane protrusions and focal adhesion dynamics during cell migration of fibroblasts. *J. Cell Biol.* 164:427–439.
- Turner, T., P. Chen, L. J. Goodly, and A. Wells. 1996. EGF receptor signaling enhances in vivo invasiveness of DU-145 human prostate carcinoma cells. *Clin. Exp. Metastasis*. 14:409–418.
- Verbeek, B. S., S. S. Adriaansen-Slot, T. M. Vroom, T. Beckers, and G. Rijkse. 1998. Overexpression of EGFR and c-erbB2 causes enhanced cell migration in human breast cancer cells and NIH3T3 fibroblasts. *FEBS Lett.* 425:145–150.
- Ware, M. F., A. Wells, and D. A. Lauffenburger. 1998. Epidermal growth factor alters fibroblast migration speed and directional persistence reciprocally and in a matrix-dependent manner. *J. Cell Sci.* 111:2423–2432.
- Weiner, O. D. 2002. Regulation of cell polarity during eukaryotic chemotaxis: the chemotactic compass. *Curr. Opin. Cell Biol.* 14:196–202.
- Wells, A., K. Gupta, P. Chang, S. Swindle, A. Glading, and H. Shiraha. 1998. Epidermal growth factor receptor-mediated motility in fibroblasts. *Microsc. Res. Tech.* 43:395–411.
- Wells, A., M. F. Ware, F. D. Allen, and D. A. Lauffenburger. 1999. Shaping up for shipping out: PLC γ signaling of morphology changes in EGF-stimulated fibroblast migration. *Cell Motil. Cytoskeleton*. 44:227–233.
- Xie, H., M. A. Pallero, D. Gupta, P. Chang, M. F. Ware, W. Witke, D. J. Kwiatkowski, D. A. Lauffenburger, J. E. Murphy-Ullrich, and A. Wells. 1998. EGF receptor regulation of cell motility: EGF induces disassembly of focal adhesions independently of the motility-associated PLC γ signaling pathway. *J. Cell Sci.* 111:615–624.